Published in final edited form as:
Physiol Behav. 2011 June 1; 103(3-4): 342–351. doi:10.1016/j.physbeh.2011.02.037.

Sexual dimorphism in locus coeruleus dendritic morphology: A structural basis for sex differences in emotional arousal

Debra Bangasser, PhD, **Xiaoyan Zhang**, **Veraaj Garachh**, **Emily Hanhauser**, and **Rita Valentino, PhD**
Department of Anesthesiology and Critical Care Medicine, Division Stress Neurobiology, The Children's Hospital of Philadelphia, Philadelphia, PA 19104

Abstract

Stress-related psychiatric disorders, such as depression and anxiety, affect a disproportionate number of women. We previously demonstrated that the major brain norepinephrine (NE)-containing nucleus, locus coeruleus (LC) is more sensitive to stressors and to the stress-related neuropeptide, corticotropin-releasing factor (CRF) in female compared to male rats. Because the LC-NE system is a stress-responsive system that is thought to be dysregulated in affective disorders, sex differences in LC structure or function could play a role in female vulnerability to these diseases. The present study used different approaches to compare LC dendritic characteristics between male and female rats. Immunofluorescence labeling of tyrosine hydroxylase, the norepinephrine synthetic enzyme, revealed that LC dendrites of female rats extend further into the peri-LC region, covering a significantly greater area than those of males. Optical density measurements of dendrites in the peri-LC revealed increased dendritic density in females compared to their male counterparts. Additionally, immunoreactivity for synaptophysin, a synaptic vesicle protein, was significantly greater in the LC in female rats, suggesting an increased number of synaptic contacts onto LC processes. Individual LC neurons were juxtacellularly labeled with neurobiotin *in vivo* for morphological analysis. LC dendritic trees of females were longer and had more branch points and ends. Consistent with this, Sholl analysis determined that, compared to males, LC dendrites of females had a more complex pattern of branching. The greater dendritic extension and complexity seen in females predicts a higher probability of communication with diverse afferents that terminate in the peri-LC. This may be a structural basis for heightened arousal in females, an effect which may, in part, account for the sex bias in incidence of stress-related psychiatric disorders.

Keywords

sex difference; dendrite; synapse; stress; affective disorder

1. Introduction

Stress-related psychiatric disorders such as depression, anxiety and post-traumatic stress disorder (PTSD) are more prevalent in women compared to men, and this has been

Corresponding author information: Debbie Bangasser, PhD, The Children's Hospital of Philadelphia, 3615 Civic Center Blvd., ARC 402E, Philadelphia, PA 19104, Phone: 215-590-0654; Fax: 215-590-3364, dbangasser@yahoo.com.

attributed to greater sensitivity of stress-responsive systems [1–7]. One stress-response system that could account for sex differences in the prevalence of stress-related psychiatric disorders is the locus coeruleus (LC)-norepinephrine (NE) system. The nucleus LC is a major source of NE in the brain and the sole source of NE in hippocampus and cortex [8, 9]. The LC-NE system mediates arousal, attention, and vigilance in response to salient stimuli [10–12]. Additionally, LC neurons are activated by stressors, resulting in NE release throughout the forebrain [13–15]. This is thought to mediate an emotional arousal limb of the stress response that is coordinated with behavioral, autonomic and endocrine components of the stress response [16, 17]. Although the LC response to acute stress is adaptive, if it extends beyond the duration of the stressor or if it occurs in the absence of stress this could be expressed as pathological hyperarousal or anxiety. LC dysregulation has been hypothesized to occur in conditions of chronic stress and has been implicated in melancholic depression and the hyperarousal and re-experiencing symptoms of PTSD [18–22]. Because these disorders occur more frequently in women than in men, it is possible that sex differences in the structure or activity of the LC-NE system, may predispose women to stress-related disorders.

One previously documented sex difference in LC structure was a larger LC composed of more neurons in female Wistar rats compared to males [23, 24]. This sex difference resulted from an increase in postpubertal proliferation of LC neurons in females and was dependent on gonadal hormones [25]. Females require a lifelong presence of estradiol for a feminized LC, whereas males require a perinatal testosterone surge for LC masculinization [23, 25–27]. However, the finding of sex differences in LC volume did not generalize to all strains or species [28–31].

More recently, we demonstrated sex differences in LC neurons at a functional level [32, 33]. Stress produced a greater activation of LC neurons in female rats and these neurons were more sensitive to the stress-related neuropeptide, corticotropin-releasing factor (CRF), which is thought to mediate activation of the LC-NE system during stress [17, 32–34]. In addition to increasing LC neuronal activity, CRF affects dendritic architecture, increasing dendritic length of LC neurons in slice cultures and promoting neurite outgrowth in LC-like CATHa cells [35, 36]. This structural effect could further influence stress vulnerability by increasing the probability of communication with brainstem and limbic afferents conveying autonomic and emotionally-related information to the LC.

The present study was designed to compare different characteristics of LC dendrites between adult male and female rats. The majority of LC inputs innervate dendrites that extend into the pericoerulear region (peri-LC) [37]. Therefore, we first determined the extent and density of LC dendrites in the peri-LC using immunofluorescence labeling for tyrosine hydroxylase (TH), the norepinephrine synthetic enzyme. To compare dendritic morphology in more detail, individual LC neurons of male and female rats were juxtacellularly labeled with neurobiotin and dendritic architecture was analyzed and compared between groups.

2. Methods

2.1 Subjects

Adult (65–85 days old) male and female Sprague-Dawley rats (Charles River, Wilmington, MA) were used. All rats had *ad libitum* access to food and water, were maintained on a 12 h light/dark cycle, and housed in same sex groups (2–3 rats/cage). For cycling females, vaginal cytology was used to track the estrous cycle as previously described [38]. For the initial study, which examined TH and synaptophysin immunoreactivity, half of the females were perfused in diestrus (characterized by low estrogen levels) while the other half were perfused in proestrus (characterized by high estrogen levels) to ensure that both hormonal

extremes were equally represented. Care and use of animals was approved by the Children's Hospital of Philadelphia's Institutional Animal Care and Use Committee and in accordance with the NIH Guide for the Care and Use of Laboratory Animals.

2.2 Immunohistochemistry for densitometry

Rats were transcardially perfused with saline 0.9% followed by 4% paraformaldehyde in 0.1 M phosphate buffer (PB). After perfusion, brains were removed, post-fixed for at least 1 h, and then stored in a 20% sucrose solution in PB with 0.1% sodium azide at 4°C for at least 48 h. Frozen coronal sections (30 μm) were cut through the LC on a cryostat and stored in either PBS for immediate processing or in cryoprotectant for long term storage.

For TH and synaptophysin immunoreactivity, every fourth section was first incubated in 0.75% H_2O_2 for 20 min and then rinsed in phosphate buffered saline (PBS) containing 0.3% Triton and 0.04% bovine serum albumin (PBS-TX-BSA) three times for 30 min. Sections were then incubated in PBS-TX-BSA and 0.1% sodium azide for 48 h at 4°C with either mouse anti-TH (1:5000, Immunostar) or rabbit anti-TH (1:2000, Millipore) and mouse anti-synaptophysin (1:75000, clone SY38, Millipore). Specificity of the anti-synaptophysin antibody has been characterized previously using a preabsorption control [39]. Sections incubated in anti-TH antibody alone were rinsed (PBS-TX-BSA) three times over 30 min and incubated in donkey anti-mouse antibody conjugated to Alexa Flour 488 (1:200, Invitrogen) for 90 min at room temperature. For dual labeling of TH and synaptophysin, sections were rinsed as described, then incubated with donkey anti-mouse antibody conjugated to Alexa Flour 594 and donkey anti-rabbit antibody conjugated to Alexa Flour 488 (1:200, Invitrogen) for 90 min at room temperature. Sections were then rinsed in PB, mounted, and cover-slipped with Fluoromount G (SouthernBiotech, Birmingham, AL, USA). Immunoreactivity was visualized by fluorescence microscopy using a Leica DMRXA microscope. Images were captured with a Hamamatsu ORCA-ER digital camera (Bridgewater, NJ, USA) using Open Laboratory software (Improvision, Coventry, UK).

2.3 Quantification of dendritic area and density

Coronal sections were selected from images of TH staining that corresponded to a rostral and mid rostrocaudal level of the LC as shown in Figure 1A. These are comparable to the zones previously described as those in which the majority of LC processes extend [40]. Previous electron microscopic studies demonstrated that nearly all of the labeled processes in these regions are dendrites [40]. Fluorescent images were taken at the same exposure, then converted to grayscale and inverted. The Image J Optical Density calibration was used to determine dendritic density in triangular regions of interest in both ventromedial and dorsolateral peri-LC regions (Fig. 1A). In addition to the density measurements, the area covered by LC dendrites in ventromedial peri-LC was outlined using Image J, and measurements were converted from pixels^2 to μm^2 for graphical presentation. To evaluate potential sex differences in TH expression, the optical density of TH in the nuclear core of the mid LC region, which contains the most cell bodies, was analyzed by outlining the portion of the LC containing only the cell bodies. For all density measurements, the mean density of a background region (taken from a portion of the image with little TH staining) was subtracted from the mean density of the region of interest and the result was multiplied by the area of the region of interest to yield the integrated density measurement. For rats with multiple rostral or mid LC sections, the data from the multiple sections were averaged (2–6 sections per animal) to yield one determination per region per animal.

Synaptophysin immunoreactivity was quantified as described above for TH. For the ventromedial and dorsolateral peri-LC regions, triangular regions of interest were used (Fig. 1A). Synaptophysin immunoreactivity was also quantified in the LC core. To this end, an

outline of the nucleus based on cell bodies as identified with TH staining was drawn and superimposed on the corresponding image of the same section that contained synaptophysin immunoreactivity. The analysis of both TH and synaptophysin immunoreactivity was performed by an individual blind to the sex of the animal.

2.4 Western blotting

Unanesthetized rats were rapidly decapitated, brains were removed, and placed in a block from which 2 mm slices containing the LC were microdissected using a trephine. LC samples were homogenized and protein concentration was determined as previously described [41]. Samples (15 μg per condition) were subjected to SDS-PAGE gel electrophoresis and proteins transferred to polyvinylidene fluoride membranes as described [33]. Probing details were as described [41] with slight modifications. Membranes were blocked with Odyssey Buffer (diluted in PBS 1:1) and incubated with mouse anti-TH (1:2000) for 90 min. Following rinsing, membranes were incubated with donkey anti-mouse IRDye 680CW (1:5000, LiCor, Lincoln, NE) for 1 h. Membranes were scanned and TH was detected using the Odyssey Infrared Imaging System (LiCor). Following quantification of the TH, membranes were incubated with rabbit anti-beta-tubulin (1:10,000) for 90 min followed by rinses and incubation with donkey anti-rabbit IRDye 800CW (1:5000, LiCor). After scanning, Odyssey Infrared Imaging software quantified the integrated intensity of each band and determined molecular weights based on Biorad Precision Plus Protein Standards. The ratio of TH to tubulin was calculated and analyzed using the Student's t-test for independent samples. For the Figures, each channel of the image was adjusted for brightness and contrast individually using the Odyssey Infrared Imaging Software.

2.5 Surgery, Electrophysiological Recording and Juxtacellular Labeling of LC Neurons

For juxtacellular labeling of individual LC neurons, rats were anesthetized with a 2% isoflurane-air mixture, positioned in a stereotaxic instrument and surgically prepared for recording extracellular single unit activity from LC neurons as previously described [33]. Neuronal activity was recorded using glass micropipettes (< 1.0 μm diameter, 10–20 MOhm) filled with neurobiotin (1.5% in sodium acetate), as previously described [42, 43]. LC neurons were tentatively identified during recording by their spontaneous discharge rates (0.5–5 Hz), entirely positive, notched waveforms (2–3 msec duration) and biphasic excitation-inhibition responses to contralateral hindpaw or tail pinch. Once activity of a putative LC neuron appeared to be stable, pulses of anodal current (200 ms, 50% duty cycle) were delivered in order to juxtacellularly label the cell [44]. The current amplitude was increased incrementally (in 0.1 nA steps) to a maximum of 10 nA until cell firing became entrained. Current intensity was adjusted to maintain entrainment without damaging the cell and the duration of labeling ranged from 15–60 s. Rats remained anesthetized for at least 1 h after labeling before transcardial perfusion.

Horizontal sections (30 μm) were cut from brains in which LC neurons were juxtacellularly labeled. Sections were incubated with mouse anti-TH as described. Then they were incubated with either rhodamine-conjugated streptavidin and fluorescein-conjugated donkey anti-mouse antiserum, or fluorescein-conjugated streptavidin and rhodamine-conjugated donkey anti-mouse antiserum (1:200, Jackson Laboratories) for 90 min at room temperature. This was followed by rinses and mounting as described above.

Filled cells and dendrites were visualized using an Olympus Fluoview FV1000 confocal microscope (Olympus, Center Valley, PA) along with Fluoview confocal software (FV10-ASW v1.7, Olympus). Neurons were imaged using a 20× objective lens and optical z-slices of 0.8 μm thick were taken to capture the entire extent of the dendritic tree.

2.6 Morphological analysis

Neurobiotin labeled LC dendrites were reconstructed and analyzed using Neurolucida (MBF Bioscience Inc., Williston, VT). Cell somas and dendrites were traced with the autoneuron feature. Dendrites were then manually edited if necessary to ensure accurate tracing. The Neurolucida Explorer program obtained measurements of the somatic volume and surface area. The dendritic parameters analyzed included the number of nodes (i.e., branch points), the number of ends, the length of the average and longest dendritic tree, and the length of the average and longest segment (i.e., distance from soma-to-node/end or node-to-node/end) (Fig. 1B). Branch order was assigned using centrifugal branch order and the number of branches and total length of branches according to branch order (i.e., primary, secondary, tertiary, etc.) was analyzed. Sholl analysis was performed by counting the number of dendrites that intersected with sholls or concentric circles that radiated from the cell body in 20 μm increments [45]. Sholls ranged from 40 μm – 280 μm, and although some dendrites exceeded 280 μm in length; 280 μm was chosen as the last Sholl because <50% of cells had dendrites that extended beyond that distance. Dendrite tracing and analysis was performed by an individual blind to the sex of the rat.

2.7 Statistical analysis

For TH and synaptophysin immunohistochemistry, an Analysis of Variance (ANOVA) was conducted that compared region (mid vs. rostral LC) and sex (i.e., 2 × 2 ANOVA). Most of the morphological characteristics were analyzed with independent samples t-tests. For analysis of dendrite order and Sholl analysis, mixed factors ANOVAs were used: the within subject factors were either branch order or Sholl length, respectively, and a between subjects factor was sex. Values that exceeded 2 SDs above or below the group mean were considered outliers and dropped from the analysis. This resulted in dropping one male and one female subject from the analysis of synaptophysin density in the dorsolateral and core regions, respectively, and one female subject from the TH westerns.

3. Results

3.1. Sex differences in the area and density of the LC dendritic field

Females were sacrificed in either diestrus or proestrus and compared to evaluate the potential contribution of circulating gonadal hormones. There was no significant difference in the LC dendritic field area between diestrus (M=154,285 μm^2 ± 22,678), and proestrus (M=170,217 μm^2 ± 23,443) females [$t(6)=0.59, p>0.05$]. Similarly, there was no significant sex difference in dendritic density in the ventromedial peri-LC between females in diestrus (M = 1,743 ± 264) and proestrus (M = 1,546 ± 433) [$t(6)= -0.39$, $p>0.05$]. In the dorsolateral peri-LC, dendritic density was also comparable between diestrus (M = 231 ± 19) and proestrus (M = 209 ± 24) females [$t(6)= 0.70$, $p>0.05$]. Therefore, data for both hormonal conditions were collapsed into one combined female group for graphical presentation and data analysis.

Figure 2 shows the LC dendritic fields in a representative male and female subject at a rostral and a mid rostrocaudal LC level comparable to levels depicted in Figure 1A. The LC dendritic field was more extensive at the mid LC level compared to the rostral LC, irrespective of the sex of the animal [$F(1,25)=10.1$, $p<0.05$, n=7–8 rats] (Figs. 2, 3A). At both rostral and mid levels, the dendritic field was larger in females compared to males [$F(1,25)=10.3$, $p<0.05$] (Fig. 3A). There was no significant interaction between LC region and sex [$F(1,25)=1.2$, $p>0.05$].

Densitometry revealed that LC dendrites in the ventromedial peri-LC were more concentrated in the mid LC versus rostral LC region, irrespective of sex [$F(1,25)=52.9$,

p<0.05, n=7–8 rats] (Fig. 3B). However, there was no regional difference in LC dendrites in the dorsolateral region [F(1,25)=2.8, p>0.05] (Fig. 3C). In both the ventromedial and dorsolateral peri-LC regions the density of dendrites was greater in females compared to males [F(1,25)=8.5, p<0.05, F(1,25)=34.6, p<0.05, ventromedial and dorsolateral, respectively] (Fig. 3B,C). There were no significant interactions between LC region and sex [F(1,25)= 2.4, p>0.05, F(1,25)= 0.3, p>0.05, ventromedial and dorsolateral, respectively].

In the same sections in which the LC dendritic area and density were quantified above, the optical density of TH in nuclear portion of the LC at a mid rostrocaudal level was found to be comparable between sexes [t(11)=0.28, p>0.05] (Fig. 3D). Additionally, Western blotting indicated that there was no sex difference in the ratio of TH:tubulin [t(22)=0.91, p>0.05, n=12] (Fig. E,F). Together these results suggest that the observed sex differences in dendritic area and density were not attributable to sex differences in TH expression.

3.2 Sex differences in synaptophysin immunoreactivity in the LC

In order to determine whether the increased LC dendritic density in female rats was accompanied by an increase in synaptic contacts onto LC dendrites, immunoreactivity for synaptophysin, a synaptic vesicle protein, was quantified. Figure 4 shows synaptophysin immunolabeling in the mid LC region in representative sections from male and female rats. Synaptophysin labeling in the ventromedial and dorsolateral peri-LC regions was comparable between mid and rostral levels [F(1,24)=0.3, p>0.05, F(1,24)=0.2, p>0.05, ventromedial and dorsolateral, respectively, n=6–8 rats] (Fig. 5A,B). However, there was more synaptophysin labeling in the mid than rostral LC core [F(1,25)=11.9, p<0.05, n=7–8 rats] (Fig. 5C). In the ventromedial peri-LC there was a trend for increased synaptophysin immunoreactivity in females compared to males [F(1,24)=3.9, p=0.059] (Fig. 5A). Females had significantly more synaptophysin labeling in the dorsolateral peri-LC than males [F(1,24)=6.2, p<0.05] (Fig. 5B). Because it is possible that the synaptophysin expression in the peri-LC regions represented synapses on dendrites from both LC neuron and non-LC neurons, synaptophysin expression was also assessed in the core of the LC where the majority of dendrites are from LC neurons. Within the nuclear core of the LC, synaptophysin immunoreactivity was greater in females than males [F(1,25)=7.8, p<0.05] (Fig. 5C). There were no significant interactions between LC region and sex [F(1,24)=0.34, p>0.05, F(1,24)=2.4, p>0.05, F(1,25)=1.0, p>0.05, ventromedial, dorsolateral and core, respectively].

3.3 Sex differences in soma size and dendritic arborizations

A total of 52 neurons were juxtacellularly labeled with neurobiotin and included 20 cells from 9 male rats and 32 cells from 12 female rats. Figure 6 shows representative examples of neurobiotin-filled TH-immunoreactive LC neurons in a male and female rat along with their Neurolucida tracings. Neurolucida analysis of the filled neurons indicated a greater somatic surface area [t(49)=2.9, p<0.05] and volume [t(49)=2.5, p<0.05] of LC neurons in males than in females (Fig. 7A).

Neurolucida analysis of LC dendrites indicated significantly more branch points (i.e., nodes) and more ends in females compared to males [t(50)=2.7, p<0.05, t(50)=2.2, p<0.05, nodes and ends, respectively] (Fig. 7B). The average length of the dendritic tree was longer in females [t(50)=2.2, p<0.05], and the size of the longest dendritic tree was greater in females than in males [t(50)=2.1, p<0.05] (Fig. 7C). Interestingly, length of the mean segment (i.e., distance from soma-to-node/end and node-to-node/end) and the length of the longest segment were comparable between males and females [t(50)=1.1, p>0.05, t(50)=1.2, p>0.05, mean and longest, respectively] (Fig. 7D). Dendrites were categorized and assessed by branch order (i.e., 1^{st},2^{nd}, 3^{rd},4^{th}, or 5^{th}). A mixed factor ANOVA revealed that neurons of

females had more branches overall [$F(1,50)=5.4$, $p<0.05$] (Fig. 7E). There were fewer higher order branches, regardless of sex [$F(4,200)=20.6$, $p<0.05$] and there was no branch order by sex interaction [$F(4,200)=2.0$, $p>0.05$]. Chi-Squared tests were used to analyze the proportion of 3rd and 4th order dendrites. While 69% of female LC neurons had 3rd order branches, only about half (55%) of male LC neurons had 3rd order branches, but the Chi-Squared analyses was not significant [χ_2 (1, $N = 52$) = 1.0, $p>0.05$]. However, LC neurons of females had a significantly greater proportion of 4th order branches (53%) than those of males (25%) [χ^2 (1, $N = 52$) = 4.0, $p<0.05$]. A similar pattern emerged when assessing the total length of the branches broken down from primary to quinary. Overall, females had longer branches than males [$F(1,50)=6.2$, $p<0.05$] (Fig. 7F). Total branch length decreased as branch order increased [$F(4,200)=83.0$, $p<0.05$] and there was no branch order by sex interaction [$F(4,200)=0.6$, $p>0.05$].

Sholl analysis was performed to assess dendritic complexity (Fig. 8A). Dendrites of females had more intersections with the Sholl circles than those of males [$F(1,50)=6.7$, $p<0.05$] (Fig. 8B). Intersections between dendrites and Sholl circles decreased further away from the cell body [$F(12,600)= 61.8$, $p<0.05$]. There was no sex by Sholl interaction [$F(12,600)=0.2$, $p>0.05$]. This analysis confirmed that females had a more complex dendritic tree than males.

4. Discussion

The present study used convergent approaches to compare LC dendritic morphology in male and female rats. TH immunoreactivity revealed that the LC dendritic field was larger and denser in females than in males. Increased synaptophysin expression in females suggested increased synapse formation with afferents in the nuclear core and dorsolateral peri-LC. Finally, morphological analysis of individually labeled LC neurons confirmed the increased complexity of LC dendrites in females compared to males. The extent of dendrites and synaptophysin expression should be related to the magnitude of afferent input processed by LC neurons. Thus, the present results suggest that LC neurons of female rats may be structured to receive and process greater amounts information. Particularly, enhanced extension into the peri-LC would increase the probability for communication with limbic afferents relaying emotionally-related information and could translate to increased expression of emotional arousal in females.

4.1 Technical considerations

A consideration in using TH-immunoreactivity as a marker of LC dendrites is the potential for sex differences in TH expression. A previous study reported a transient increase in TH expression in the LC of young adult (60 day) female C57BL/6J mice [46]. However, in the present study we found no sex difference in the density of TH immunoreactivity in nuclear core of the LC in Sprague-Dawley rats and this was confirmed in Western blots. Importantly, the findings from the analysis of TH-immunoreactivity were verified using neurobiotin labeling of individual LC neurons. Thus, the increased dendritic density observed in females is not due to sex differences in TH expression, but rather sex differences in dendritic structure.

4.2 Sex differences in LC neuronal morphology

Previous studies have found sex differences in structural characteristics of the LC. The LC nucleus is larger in volume and is composed of more neurons with larger somas in female Wistar rats compared to males [23, 24]. However, sex differences in LC volume and cell number are not apparent in all strains or species [28–31]. In fact, in Sprague-Dawley rats the dorsal LC is actually smaller in females compared to males [31]. Consistent with this, the

present study found that, unlike Wistar rats, LC somas of female Sprague-Dawley rats were smaller than those of males.

The results of the present study are the first, to our knowledge, to demonstrate sex differences in LC dendritic characteristics. One major finding was that the density of dendrites in both the ventromedial and dorsolateral peri-LC regions was greater in females than males. Because the number of LC neurons in some rat strains is greater in females, it is possible that this increased dendritic density reflects an increase in the total number of neurons rather than an increase in the complexity of individual LC dendritic trees [23, 24, 28, 29]. However, morphological analysis of individual juxtacellularly labeled LC neurons revealed that LC neurons of females had a more complex dendritic morphology, arguing that this contributes, at least in part, to the higher density of dendrites in a particular region observed in females.

Interestingly, the length of the individual dendrite segments (i.e., distance from soma-to-node/end, node-to-node/end) was comparable between males and females, indicating that the more extensive dendritic tree in females was due to an increased number of branch points and higher order branching, rather than an increase in the length of individual segments. This distinction between more branches versus longer segments implicates specific regulatory mechanisms in establishing this sex difference. For example, certain Rho GTPases, such as Rac1 and Cdc42, increase dendritic branching, whereas RhoA controls dendrite length [47]. The present findings would suggest sex differences in the function Rac1 and/or Cdc42 rather than RhoA.

4.3 Factors that may establish this sex difference

The sex differences in LC dendritic structure could be established by gonadal hormones, which have been shown to regulate dendritic growth and complexity of other neurons (e.g., [48–52]. For example, estrogen promotes dendritic growth of cerebellar cells and branching of hippocampal dendrites [50, 51]. In this present study, sex differences in LC dendrites were not related to estrous cycle stages, suggesting that the pubertal estrogen surge, rather than circulating levels, could establish this difference. Alternatively, testosterone, which surges in the perinatal and pubertal periods in males, may play a critical role. The pubertal testosterone surge is associated with dendritic pruning in the medial amygdala, so a similar mechanism could explain the reduced dendritic tree in LC neurons of males [52]. Finally, some sex differences arise because of the differential representation of genes on the X and Y chromosomes in non-gonadal cells [53, 54]. Thus, it is possible that genes on the X and Y chromosomes, rather than gonadal hormones, mediate the sex difference in LC dendritic morphology.

Another potential mediator of sex differences in LC dendritic structure is the stress-related neuropeptide, CRF. CRF promotes neurite outgrowth in LC-like CATHa cells through a MAP kinase-dependent process [36]. In organotypic slice cultures, CRF accelerated the growth of LC dendrites and increased branch length [35]. These effects required activation of the CRF_1 receptor, protein kinase A and Rac1 [35]. In addition to its structural effects on LC neurons, CRF increases LC neuronal discharge rate and this response also requires CRF_1 activation and cyclic AMP/protein kinase A signaling [32, 55, 56]. LC neurons of female rats are more sensitive to this CRF effect as a result of enhanced CRF_1 receptor association with the GTP-binding protein G_s and subsequent activation of cyclic AMP signaling/ protein kinase A cascade, the same signaling cascade thought to be involved in the structural effects of CRF [32, 33]. Because the physiological and structural effects of CRF on LC neurons are mediated by a common receptor and at least the initial components of the signaling cascade, increased coupling of CRF_1 to G_s in females could account for sexual dimorphism of LC dendritic structure.

4.4 Functional implications

The relevance of a more extensive LC dendritic tree in females lies in the topographical pattern of LC afferent terminations. In contrast to its widespread efferent system, the nuclear LC receives input that is restricted to the nucleus paragigantoceullaris, the nucleus prepositus hypoglossi, Barrington's nucleus and the dorsal cap of the paraventricular hypothalamic nucleus [37, 57, 58]. However, the LC can receive communication from other nuclei whose axons terminate in the peri-LC where they can synapse with LC dendrites that extend for hundreds of microns outside of the nucleus [40]. For example, the LC can receive autonomic information from axons of the nucleus of the solitary tract that terminate in the ventromedial peri-LC [37]. Axons from the periaqueductal gray also terminate in the ventromedial peri-LC, providing a mechanism for relaying nociceptive information [37]. Limbic afferents from central nucleus of the amygdala and bed nucleus of the stria terminalis terminate within the dorsolateral peri-LC [16, 59]. Their communication with the LC may coordinate an arousal response with autonomic and behavioral responses to emotionally-related stimuli. The more LC dendrites extend into the peri-LC, the greater the probability of synaptic contacts with the unique population of peri-LC afferents. This design would allow the LC of females to process more diverse and particularly, emotion-related, information. This could be adaptive for promoting bonding to, caring for and protecting offspring. Outside of this context however, heightened emotional arousal can be expressed as pathology, such as, increased stress or pain reactivity in females. Stress-related psychiatric disorders, which are more prevalent in females, are thought to involve overactivation of both limbic and LC-NE systems. For example, in patients with PTSD and depression, heightened amygdala activity is reported [60, 61]. Moreover, activation of the LC-NE system is thought to contribute to the hyperarousal and re-experiencing symptoms of PTSD, as well as to the hyperarousal, insomnia, and loss of appetite that characterize melancholic depression [18–22]. Thus, despite the fact that the greater complexity of LC dendrites in females is potentially adaptive in some circumstances, this sex difference may also play a role in the increased incidence of these stress-related psychiatric disorders in females.

5. Conclusions

Overall the results of the present study demonstrate that LC dendrites of females are longer and more complex than those of males. This would increase the probability for communication with the diverse and unique set of afferents that terminate in the peri-LC. This includes limbic afferents that relay emotionally-related information. Because the LC mediates arousal and attention in response to stimuli and challenges in a dynamic environment, this structural sex difference in LC dendrites may translate to a heightened emotional arousal response that can be adaptive. However, as hyperarousal is a symptom of stress-related psychiatric disorders, this structural difference also may contribute to the higher rates of these disorders in women.

Acknowledgments

This work was supported by USPHS Grant MH40008 to RJV and MH014654 and MH084423 to DAB.

References

1. Kessler RC, McGonagle KA, Swartz M, Blazer DG, Nelson CB. Sex and depression in the National Comorbidity Survey. I: Lifetime prevalence, chronicity and recurrence. J Affect Disord. 1993; 29:85–96. [PubMed: 8300981]
2. Kessler RC, Sonnega A, Bromet E, Hughes M, Nelson CB. Posttraumatic stress disorder in the National Comorbidity Survey. Arch Gen Psychiatry. 1995; 52:1048–1060. [PubMed: 7492257]

3. Marcus SM, Young EA, Kerber KB, Kornstein S, Farabaugh AH, Mitchell J, et al. Gender differences in depression: findings from the STAR*D study. J Affect Disord. 2005; 87:141–150. [PubMed: 15982748]
4. Ter Horst GJ, Wichmann R, Gerrits M, Westenbroek C, Lin Y. Sex differences in stress responses: focus on ovarian hormones. Physiol Behav. 2009; 97:239–249. [PubMed: 19275910]
5. Young EA, Altemus M. Puberty, ovarian steroids, and stress. Ann N Y Acad Sci. 2004; 1021:124–133. [PubMed: 15251881]
6. Young EA. Sex differences in response to exogenous corticosterone: a rat model of hypercortisolemia. Mol Psychiatry. 1996; 1:313–319. [PubMed: 9118357]
7. Young EA, Ribeiro SC, Ye W. Sex differences in ACTH pulsatility following metyrapone blockade in patients with major depression. Psychoneuroendocrinology. 2007; 32:503–507. [PubMed: 17462829]
8. Aston-Jones, G.; Shipley, MT.; Grzanna, R. The locus coeruleus, A5 and A7 noradrenergic cell groups. In: Paxinos, G., editor. The Rat Brain. Academic Press; 1995. p. 183-213.
9. Swanson LW, Hartman BK. The central adrenergic system. An immunofluorescence study of the location of cell bodies and their efferent connections in the rat utilizing dopamine-beta-hydroxylase as a marker. J Comp Neurol. 1975; 163:467–505. [PubMed: 1100685]
10. Aston-Jones G, Rajkowski J, Cohen J. Locus coeruleus and regulation of behavioral flexibility and attention. Prog Brain Res. 2000; 126:165–182. [PubMed: 11105646]
11. Berridge CW, Waterhouse BD. The locus coeruleus-noradrenergic system: modulation of behavioral state and state-dependent cognitive processes. Brain Res Brain Res Rev. 2003; 42:33–84. [PubMed: 12668290]
12. Bouret S, Sara SJ. Network reset: a simplified overarching theory of locus coeruleus noradrenaline function. Trends Neurosci. 2005; 28:574–582. [PubMed: 16165227]
13. Abercrombie ED, Keller RW, Zigmond MJ. Characterization of hippocampal norepinephrine release as measured by microdialysis perfusion: pharmacological and behavioral studies. Neuroscience. 1988; 27:897–904. [PubMed: 3252176]
14. Britton KT, Segal DS, Kuczenski R, Hauger R. Dissociation between in vivo hippocampal norepinephrine response and behavioral/neuroendocrine responses to noise stress in rats. Brain Res. 1992; 574:125–130. [PubMed: 1638389]
15. Smagin GN, Swiergiel AH, Dunn AJ. Sodium nitroprusside infusions activate cortical and hypothalamic noradrenergic systems in rats. Neurosci. Res. Comm. 1994; 14:85–91.
16. Van Bockstaele EJ, Colago EE, Valentino RJ. Amygdaloid corticotropin-releasing factor targets locus coeruleus dendrites: substrate for the co-ordination of emotional and cognitive limbs of the stress response. J Neuroendocrinol. 1998; 10:743–757. [PubMed: 9792326]
17. Valentino RJ, Van Bockstaele E. Convergent regulation of locus coeruleus activity as an adaptive response to stress. Eur J Pharmacol. 2008; 583:194–203. [PubMed: 18255055]
18. Wong ML, Kling MA, Munson PJ, Listwak S, Licinio J, Prolo P, et al. Pronounced and sustained central hypernoradrenergic function in major depression with melancholic features: relation to hypercortisolism and corticotropin-releasing hormone. Proc Natl Acad Sci U S A. 2000; 97:325–330. [PubMed: 10618417]
19. Gold PW, Wong ML, Chrousos GP, Licinio J. Stress system abnormalities in melancholic and atypical depression: molecular, pathophysiological, and therapeutic implications. Mol Psychiatry. 1996; 1:257–264. [PubMed: 9118349]
20. Gold PW, Chrousos GP. Organization of the stress system and its dysregulation in melancholic and atypical depression: high vs low CRH/NE states. Mol Psychiatry. 2002; 7:254–275. [PubMed: 11920153]
21. O'Donnell T, Hegadoren KM, Coupland NC. Noradrenergic mechanisms in the pathophysiology of post-traumatic stress disorder. Neuropsychobiology. 2004; 50:273–283. [PubMed: 15539856]
22. Southwick SM, Bremner JD, Rasmusson A, Morgan CA 3rd, Arnsten A, Charney DS. Role of norepinephrine in the pathophysiology and treatment of posttraumatic stress disorder. Biol Psychiatry. 1999; 46:1192–1204. [PubMed: 10560025]
23. Guillamon A, de Blas MR, Segovia S. Effects of sex steroids on the development of the locus coeruleus in the rat. Brain Res. 1988; 468:306–310. [PubMed: 3382961]

24. Luque JM, de Blas MR, Segovia S, Guillamon A. Sexual dimorphism of the dopamine-beta-hydroxylase-immunoreactive neurons in the rat locus ceruleus. Brain Res Dev Brain Res. 1992; 67:211–215.
25. Pinos H, Collado P, Rodriguez-Zafra M, Rodriguez C, Segovia S, Guillamon A. The development of sex differences in the locus coeruleus of the rat. Brain Res Bull. 2001; 56:73–78. [PubMed: 11604252]
26. Rodriguez-Zafra M, De Blas MR, Perez-Laso C, Cales JM, Guillamon A, Segovia S. Effects of perinatal diazepam exposure on the sexually dimorphic rat locus coeruleus. Neurotoxicol Teratol. 1993; 15:139–144. [PubMed: 8510608]
27. Segovia S, Perez-Laso C, Rodriguez-Zafra M, Cales JM, Del Abril A, De Blas MR, et al. Early postnatal diazepam exposure alters sex differences in the rat brain. Brain Res Bull. 1991; 26:899–907. [PubMed: 1933410]
28. Garcia-Falgueras A, Pinos H, Fernandez R, Collado P, Pasaro E, Segovia S, et al. Sexual dimorphism in hybrids rats. Brain Res. 2006; 1123:42–50. [PubMed: 17070787]
29. Garcia-Falgueras A, Pinos H, Collado P, Pasaro E, Fernandez R, Segovia S, et al. The expression of brain sexual dimorphism in artificial selection of rat strains. Brain Res. 2005; 1052:130–138. [PubMed: 16024003]
30. Segovia S, Garcia-Falgueras A, Carrillo B, Collado P, Pinos H, Perez-Laso C, et al. Sexual dimorphism in the vomeronasal system of the rabbit. Brain Res. 2006; 1102:52–62. [PubMed: 16806123]
31. Babstock D, Malsbury CW, Harley CW. The dorsal locus coeruleus is larger in male than in female Sprague-Dawley rats. Neurosci Lett. 1997; 224:157–160. [PubMed: 9131660]
32. Bangasser DA, Curtis A, Reyes BA, Bethea TT, Parastatidis I, Ischiropoulos H, et al. Sex differences in corticotropin-releasing factor receptor signaling and trafficking: potential role in female vulnerability to stress-related psychopathology. Mol Psychiatry. 2010; 15:877, 96–904. [PubMed: 20548297]
33. Curtis AL, Bethea T, Valentino RJ. Sexually dimorphic responses of the brain norepinephrine system to stress and corticotropin-releasing factor. Neuropsychopharmacology. 2006; 31:544–554. [PubMed: 16123744]
34. Valentino RJ, Page ME, Curtis AL. Activation of noradrenergic locus coeruleus neurons by hemodynamic stress is due to local release of corticotropin-releasing factor. Brain Res. 1991; 555:25–34. [PubMed: 1933327]
35. Swinny JD, Valentino RJ. Corticotropin-releasing factor promotes growth of brain norepinephrine neuronal processes through Rho GTPase regulators of the actin cytoskeleton in rat. Eur J Neurosci. 2006; 24:2481–2490. [PubMed: 17100837]
36. Cibelli G, Corsi P, Diana G, Vitiello F, Thiel G. Corticotropin-releasing factor triggers neurite outgrowth of a catecholaminergic immortalized neuron via cAMP and MAP kinase signalling pathways. Eur J Neurosci. 2001; 13:1339–1348. [PubMed: 11298794]
37. Van Bockstaele EJ, Bajic D, Proudfit H, Valentino RJ. Topographic architecture of stress-related pathways targeting the noradrenergic locus coeruleus. Physiol. and Behav. 2001; 73:273–283. [PubMed: 11438352]
38. Bangasser DA, Shors TJ. The bed nucleus of the stria terminalis modulates learning after stress in masculinized but not cycling females. J Neurosci. 2008; 28:6383–6387. [PubMed: 18562608]
39. Shigematsu K, Nishida N, Sakai H, Igawa T, Toriyama K, Nakatani A, et al. Synaptophysin immunoreactivity in adrenocortical adenomas: a correlation between synaptophysin and CYP17A1 expression. Eur J Endocrinol. 2009; 161:939–945. [PubMed: 19755404]
40. Shipley MT, Fu L, Ennis M, Liu W, Aston-Jones G. Dendrites of locus coeruleus neurons extend preferentially into two pericoerulear zones. J. Comp. Neurol. 1996; 365:56–68. [PubMed: 8821441]
41. Carr GV, Bangasser DA, Bethea T, Young M, Valentino RJ, Lucki I. Antidepressant-Like Effects of kappa-Opioid Receptor Antagonists in Wistar Kyoto Rats. Neuropsychopharmacology. 2009
42. Pernar L, Curtis AL, Vale WW, Rivier JE, Valentino RJ. Selective activation of corticotropin-releasing factor-2 receptors on neurochemically identified neurons in the rat dorsal raphe nucleus reveals dual actions. J Neurosci. 2004; 24:1305–1311. [PubMed: 14960601]

43. Rouzade-Dominguez ML, Pernar L, Beck S, Valentino RJ. Convergent responses of Barrington's nucleus neurons to pelvic visceral stimuli in the rat: a juxtacellular labelling study. Eur J Neurosci. 2003; 18:3325–3334. [PubMed: 14686905]
44. Schreihofer AM, Guyenet PG. Identification of C1 presympathetic neurons in rat rostral ventrolateral medulla by juxtacellular labeling in vivo. J. Comp. Neurol. 1997; 387:524–536. [PubMed: 9373011]
45. Sholl DA. Dendritic organization in the neurons of the visual and motor cortices of the cat. J Anat. 1953; 87:387–406. [PubMed: 13117757]
46. Pendergast JS, Tuesta LM, Bethea JR. Oestrogen receptor beta contributes to the transient sex difference in tyrosine hydroxylase expression in the mouse locus coeruleus. J Neuroendocrinol. 2008; 20:1155–1164. [PubMed: 18680559]
47. Van Aelst L, Cline HT. Rho GTPases and activity-dependent dendrite development. Curr Opin Neurobiol. 2004; 14:297–304. [PubMed: 15194109]
48. Rand MN, Breedlove SM. Androgen alters the dendritic arbors of SNB motoneurons by acting upon their target muscles. J Neurosci. 1995; 15:4408–4416. [PubMed: 7540674]
49. Griffin GD, Flanagan-Cato LM. Sex differences in the dendritic arbor of hypothalamic ventromedial nucleus neurons. Physiol Behav. 2009; 97:151–156. [PubMed: 19254731]
50. Audesirk T, Cabell L, Kern M, Audesirk G. beta-estradiol influences differentiation of hippocampal neurons in vitro through an estrogen receptor-mediated process. Neuroscience. 2003; 121:927–934. [PubMed: 14580943]
51. Sasahara K, Shikimi H, Haraguchi S, Sakamoto H, Honda S, Harada N, et al. Mode of action and functional significance of estrogen-inducing dendritic growth, spinogenesis, and synaptogenesis in the developing Purkinje cell. J Neurosci. 2007; 27:7408–7417. [PubMed: 17626201]
52. Zehr JL, Todd BJ, Schulz KM, McCarthy MM, Sisk CL. Dendritic pruning of the medial amygdala during pubertal development of the male Syrian hamster. J Neurobiol. 2006; 66:578–590. [PubMed: 16555234]
53. De Vries GJ, Rissman EF, Simerly RB, Yang LY, Scordalakes EM, Auger CJ, et al. A model system for study of sex chromosome effects on sexually dimorphic neural and behavioral traits. J Neurosci. 2002; 22:9005–9014. [PubMed: 12388607]
54. Arnold AP. Sex chromosomes and brain gender. Nat Rev Neurosci. 2004; 5:701–708. [PubMed: 15322528]
55. Schulz DW, Mansbach RS, Sprouse J, Braselton JP, Collins J, Corman M, et al. CP-154,526: a potent and selective nonpeptide antagonist of corticotropin releasing factor receptors. Proc Natl Acad Sci U S A. 1996; 93:10477–10482. [PubMed: 8816826]
56. Jedema HP, Grace AA. Corticotropin-releasing hormone directly activates noradrenergic neurons of the locus ceruleus recorded in vitro. J Neurosci. 2004; 24:9703–9713. [PubMed: 15509759]
57. Aston-Jones G, Ennis M, Pieribone VA, Nickell WT, Shipley MT. The brain nucleus locus coeruleus: restricted afferent control of a broad efferent network. Science. 1986; 234:734–737. [PubMed: 3775363]
58. Valentino RJ, Chen S, Zhu Y, Aston-Jones G. Evidence for divergent projections of corticotropin-releasing hormone neurons of Barrington's nucleus to the locus coeruleus and spinal cord. Brain Res. 1996; 732:1–15. [PubMed: 8891263]
59. Van Bockstaele EJ, Colago EE, Valentino RJ. Corticotropin-releasing factor-containing axon terminals synapse onto catecholamine dendrites and may presynaptically modulate other afferents in the rostral pole of the nucleus locus coeruleus in the rat brain. J Comp Neurol. 1996; 364:523–534. [PubMed: 8820881]
60. Victor TA, Furey ML, Fromm SJ, Ohman A, Drevets WC. Relationship between amygdala responses to masked faces and mood state and treatment in major depressive disorder. Arch Gen Psychiatry. 67:1128–1138. [PubMed: 21041614]
61. Brohawn KH, Offringa R, Pfaff DL, Hughes KC, Shin LM. The neural correlates of emotional memory in posttraumatic stress disorder. Biol Psychiatry. 68:1023–1030. [PubMed: 20855060]
62. Paxinos, G.; Watson, C. The Rat Brain in Stereotaxic Coordinates. 2nd ed. North Ryde: Academic Press; 1998.

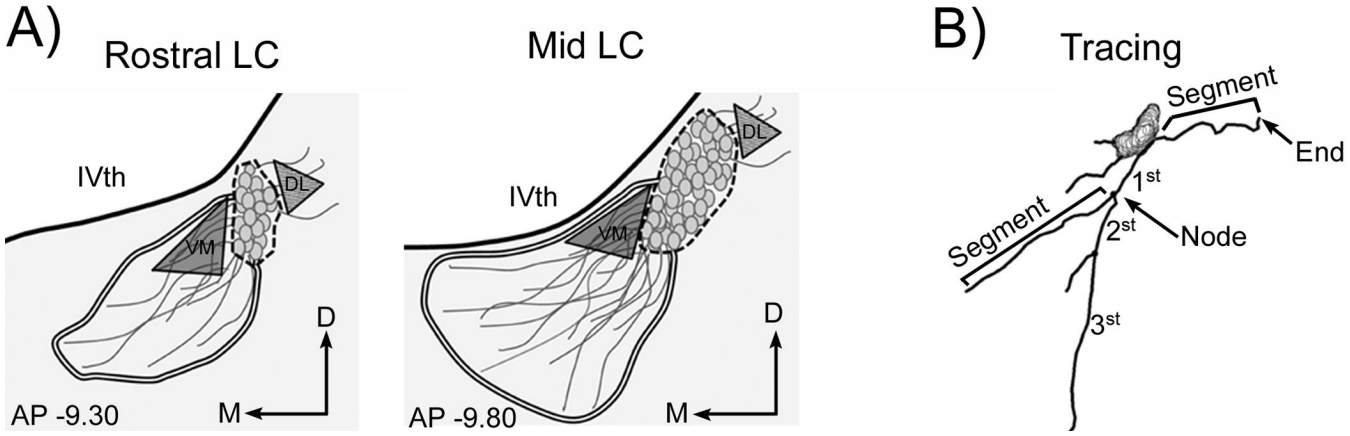

Figure 1.

Diagrams depict endpoints analyzed for densitometry and morphology. (A) Schematics represent the regions sampled in a level of the rostral LC (left) and a middle level of the rostrocaudal LC (right). The rostral and mid LC regions are AP −9.30 and −9.80 relative to Bregma, respectively [62]. The nuclear core (i.e., LC cell bodies) is defined by the dashed line. The double line demarcates the area of the ventromedial dendrites analyzed. The shaded triangle represents the region of interest used to assess the density of the ventromedial dendrites. The striped triangle represents the region of interested used to assess the density of the dorsolateral dendrites. (B) Shown on the representative trace are examples of an end, a node, and segments. This neuron also had primary (1st), secondary (2nd), and tertiary dendrites (3rd). Abbreviations: IVth, fourth ventricle; D, dorsal; DL, dorsolateral; M, medial; VM, ventromedial

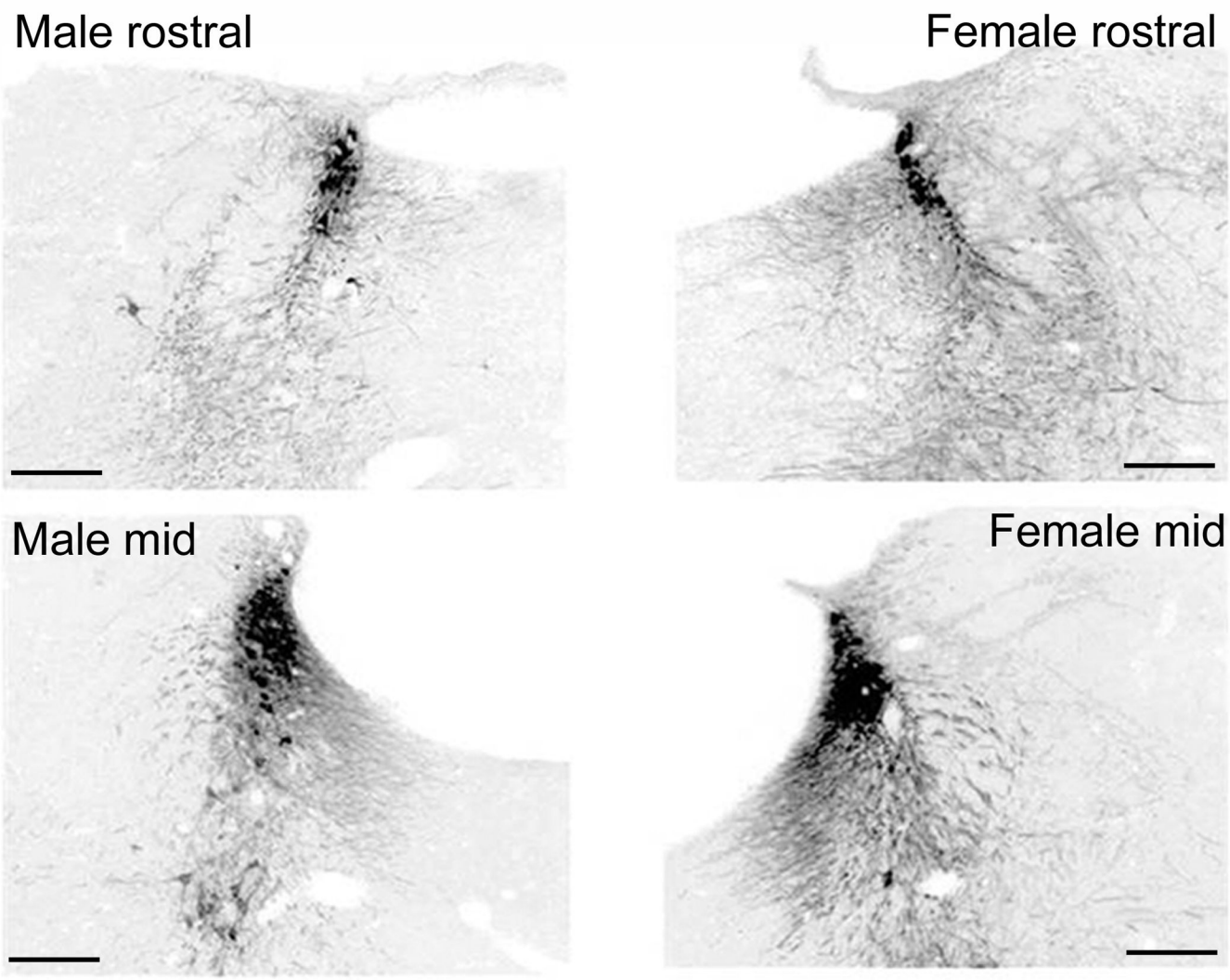

Figure 2.
Comparison of the TH-immunofluorescence in the LC and peri-LC of a male and female rat. Photomicrographs of coronal sections at the level of the rostral (top) and mid LC (bottom) of a male (left) and female (right) rat. Grayscale images of TH-immunofluorescence were inverted for quantification. Scale bars = 200 μm.

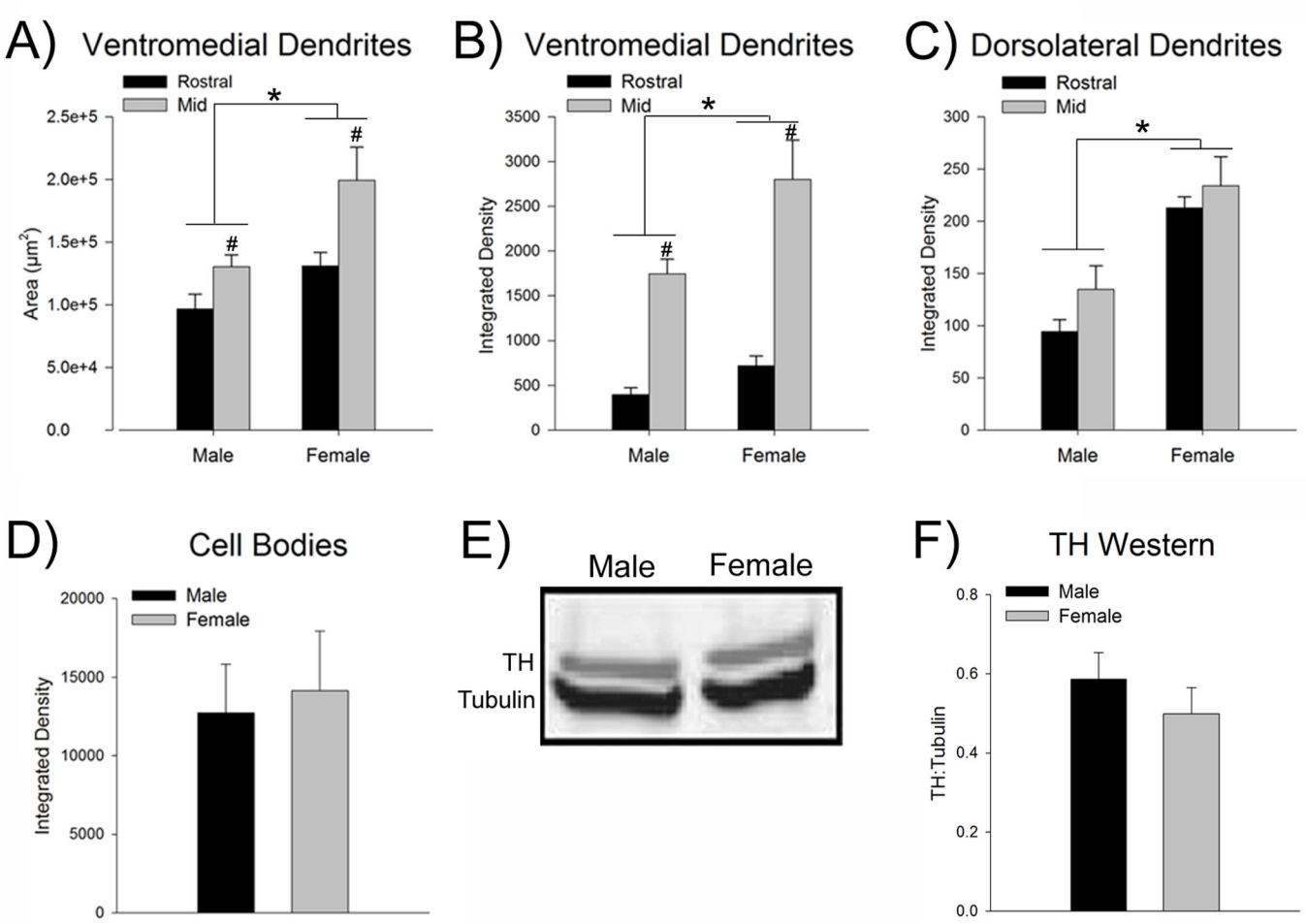

Figure 3.

The LC dendritic field is more extensive and LC dendrites are denser in female rats. (A) Bars show the mean total area (μm^2) covered by dendrites in the ventromedial peri-LC region. This area is more extensive in females than in males (n=7–8). (B) Bars show the mean optical integrated density of LC dendrites the ventromedial region. Compared to males, the density of dendrites in this area was greater in female rats. (C) Bars show the mean dendritic density in the dorsolateral peri-LC region, which was greater in females than in males. (D) Bars show the mean integrated density of TH expression in the cell body region of the mid LC (n=6–7). There was no sex difference in TH expression in LC cell bodies. (E) Representative Western blot of TH (top bands, MW = 58) and tubulin (bottom bands, MW = 51) from a representative male (left) and female (right) rat. Blots have been inverted and converted to grayscale for presentation. (F) Bars represent the mean amount of TH protein normalized to a tubulin loading control from LC punches taken from male and female rats (n=12). There was no sex difference in the level of TH protein. Asterisks indicate a significant main effect of sex ($p<0.05$). Number signs indicate a significant main effect of region ($p<0.05$). Data are represented as the mean (±s.e.m.).

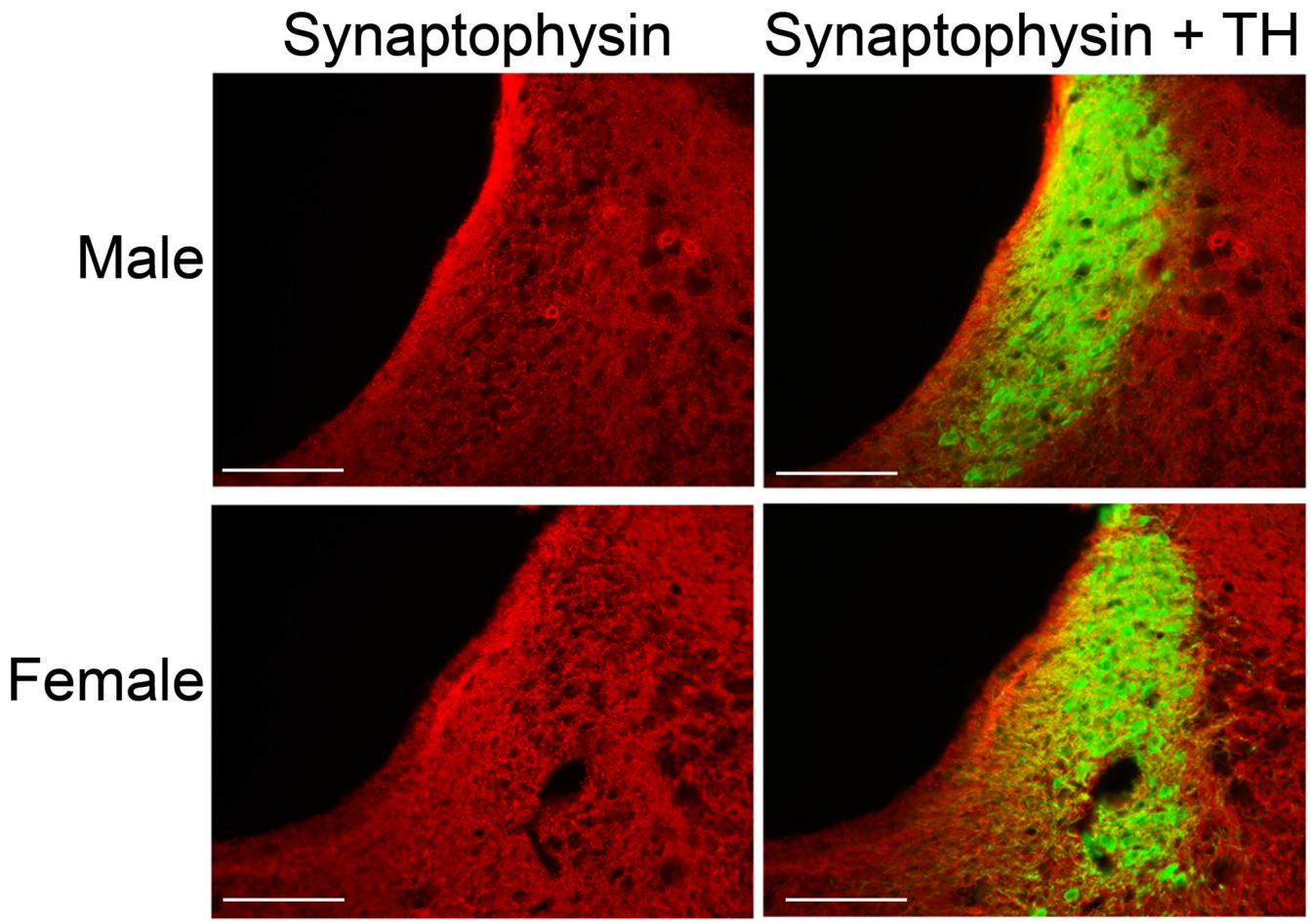

Figure 4.
Comparison of synaptophysin immunoreactivity in the LC of male and female rats. Photomicrographs of coronal mid LC sections showing synaptophysin immunoreactivity (red, middle) and the merged image of synaptophysin and TH immunoreactivity (green, right). A representative male is shown in the top row and a representative female is shown on the bottom row. Scale bars = 200 μm.

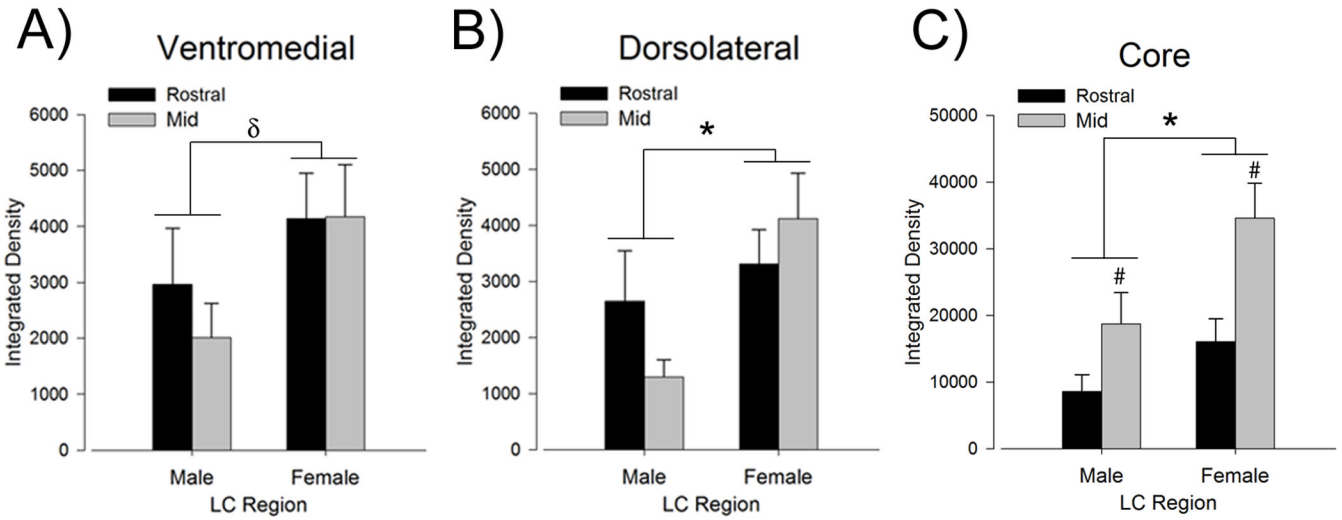

Figure 5.

Quantification of synpatophysin labeling reveals increased density in the LC and peri-LC of female rats. (A–C) Bars represent the mean integrated density of synaptophysin immunoreactivity in the ventromedial peri-LC (A), dorsolateral peri-LC (B), and core (C) (n=6–8). Asterisks indicate a significant main effect of sex ($p<0.05$). Number signs indicate a significant main effect of region ($p<0.05$). Delta indicates a trend for a sex difference ($p=0.06$). Data are represented as the mean (±s.e.m.).

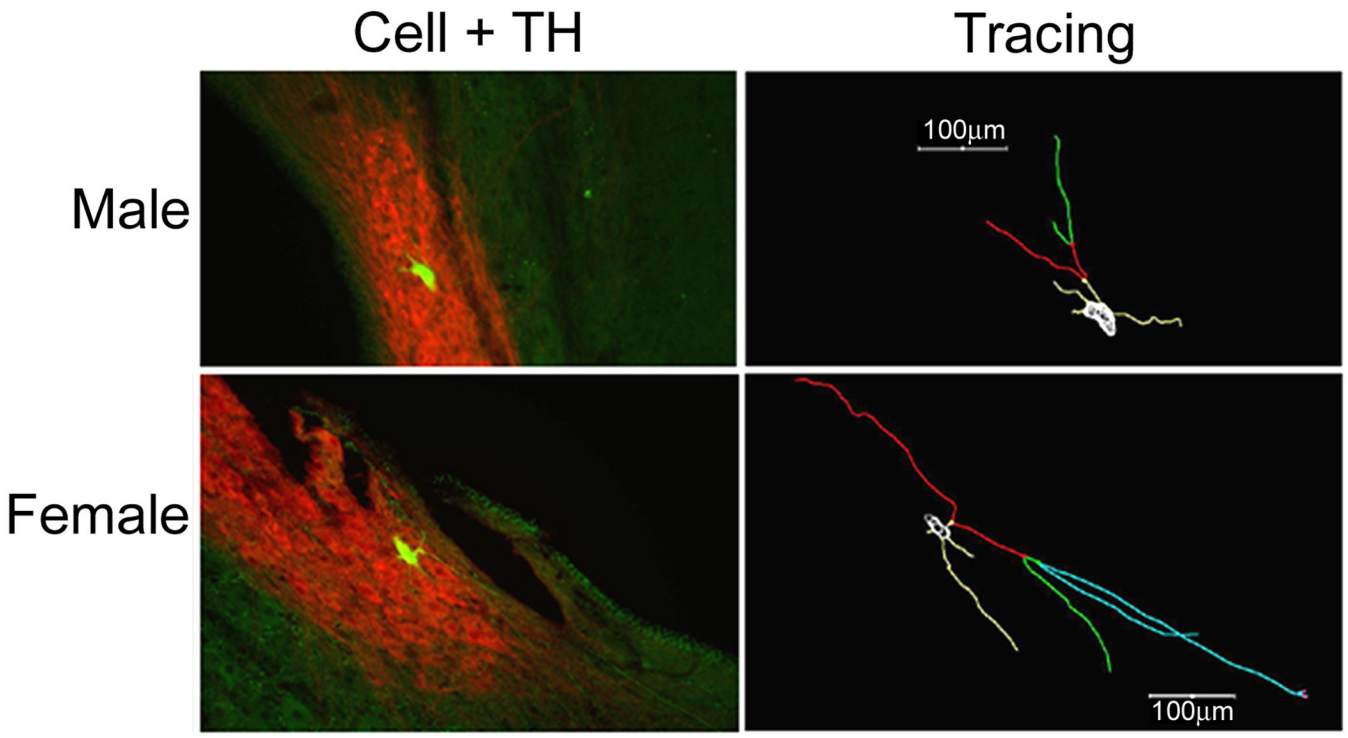

Figure 6.
Comparison of individual neurobiotin labeled LC neurons in a male and female rat. Fluorescent photomicrograph (left) of a neurobiotin labeled LC cell (green) merged with TH (red), and the corresponding cell tracing (right). Branches on the tracing are colored according to branch order (1st is yellow, 2nd is red, 3rd is green, 4th is blue, and 5th is pink). A representative male is shown in the top row, while a representative female is shown on the bottom row.

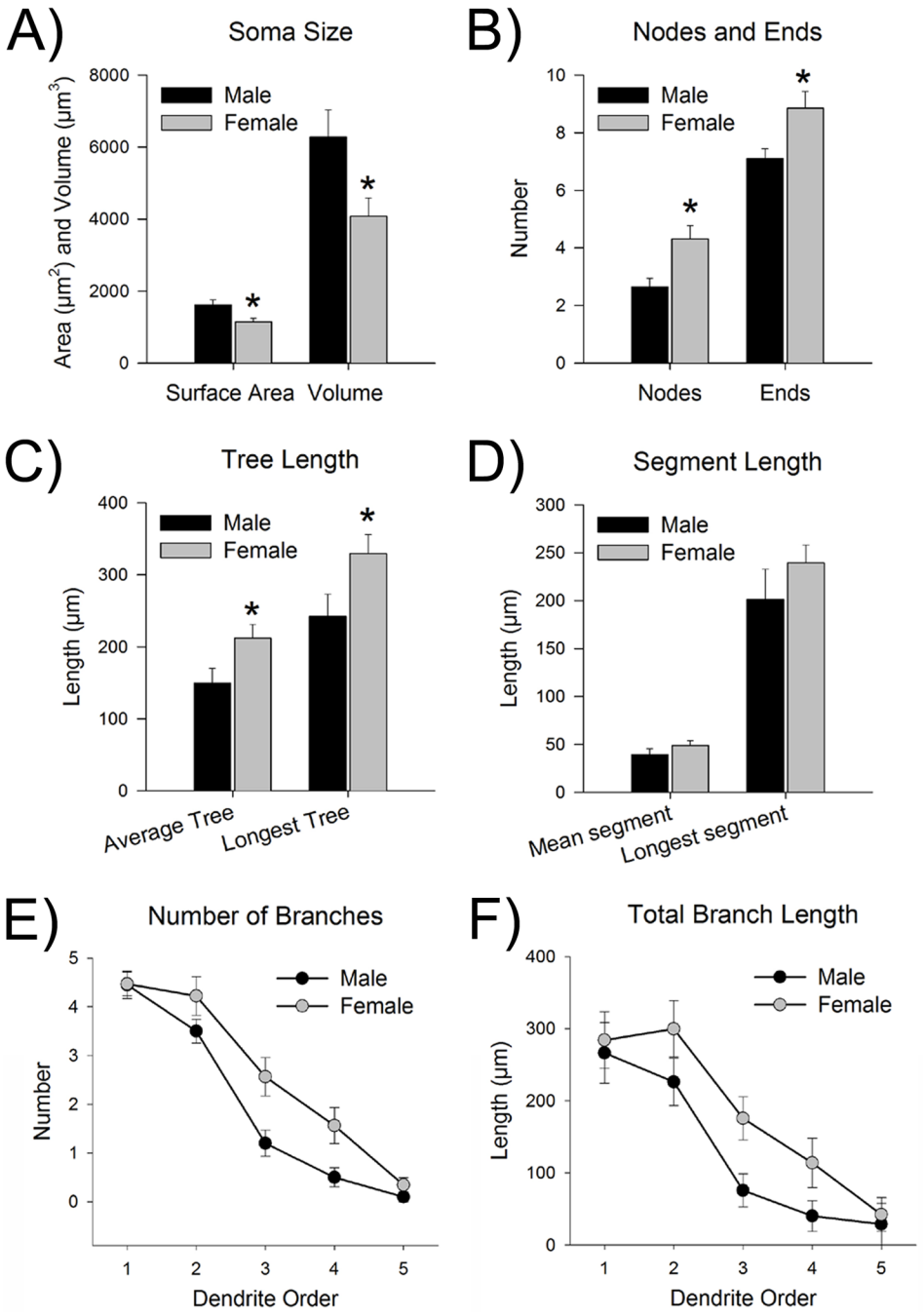

Figure 7.

Morphological analysis revealed that dendrites of females had more branches than those of males. (A) The left bars represent the surface area (μm^2) of the somas, while the right bars represent soma volume (μm^3). Both measurements indicate that males (black bars, n=19–20 cells from 9 male rats) had larger somas than females (gray bars, n=32 cells from 12 female rats). (B) The left bars represent the number of nodes (i.e., branch points) on the dendrites, while the right bars represent the number of ends. Dendrites of females had more nodes and ends, indicative of increased branching. (C) The left bar shows the length of the average dendritic tree, while the right bars show the length of the longest dendritic tree. The dendritic trees of females were significantly longer than those of males. (D) The left bars

display the length of the average segment, while the right bars display the length of the longest segment. Segment length was comparable between male and female dendrites. (E) The graph represents the number of branches broken down by branch order (i.e., 1st, 2nd, 3rd, 4th, and 5th). Dendrites of females had significantly more branches, regardless of branch order, than males. (F) The graph represents the length of branches broken down by branch order. Dendrites of females were significantly longer than those of males, regardless of branch order. Data are represented as the mean (±s.e.m.). Asterisks indicate a significant sex difference ($p<0.05$).

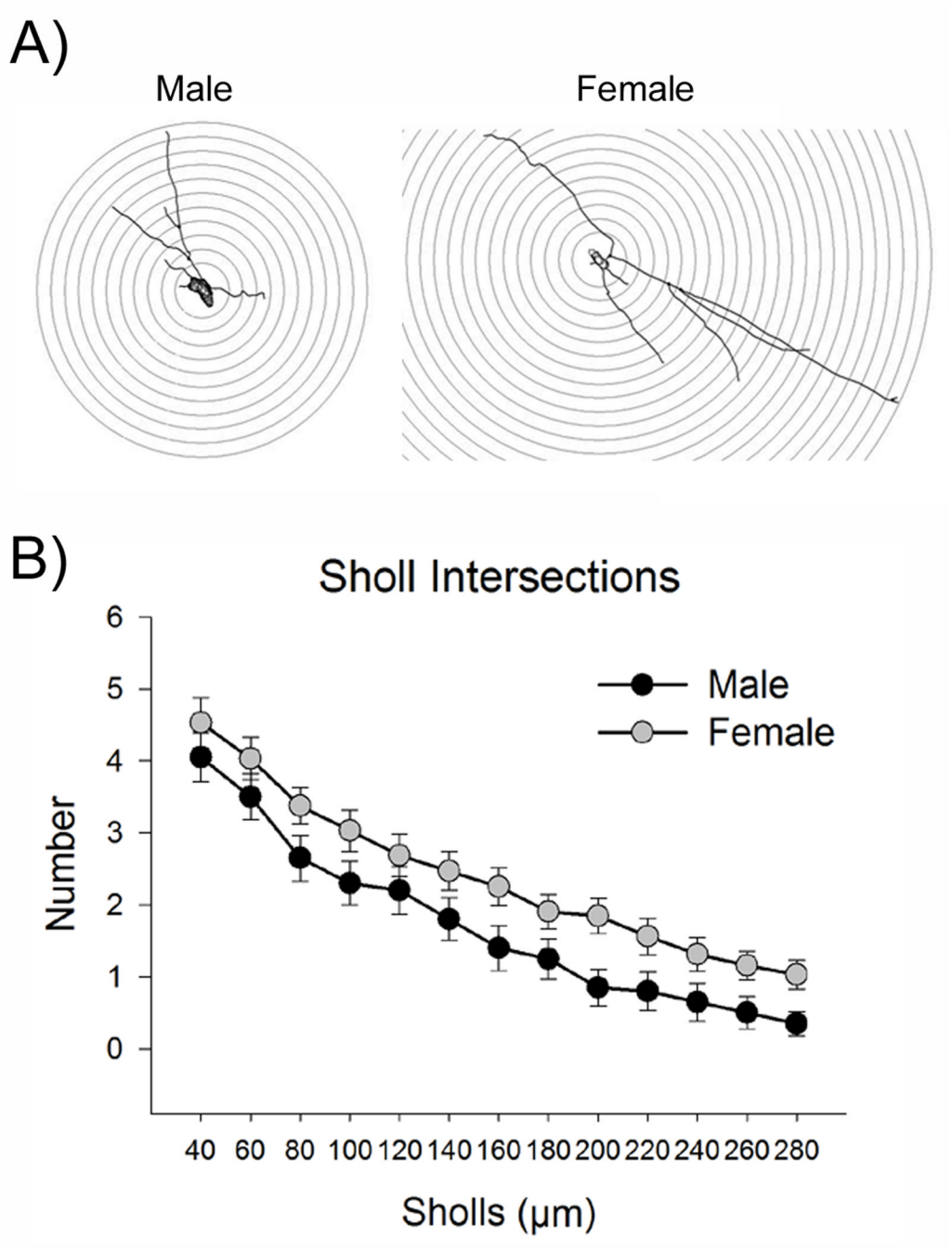

Figure 8.

Sholl analysis revealed increased complexity of LC dendrites in females. (A) This is a diagram of a Sholl analysis of a representative tracing from a male (left) and female rat (right). Concentric Sholls were placed so that they radiated in 20 μm increments from around the cell body. Intersections with these Sholls were counted. (B) This graph displays the number of intersections with the Sholls at increasing distances from the cell body. Dendrites of females (n=32 cells from 12 female rats) intersected with more Sholls than those of males (n=20 cells from 9 male rats), indicating that the female dendritic tree was more complex.